

# Genetic characterization of p27<sup>kip1</sup> and stathmin in controlling cell proliferation in vivo

Stefania Berton<sup>1,†</sup>, Ilenia Pellizzari<sup>1,†</sup>, Linda Fabris<sup>1,†</sup>, Sara D'Andrea<sup>1</sup>, Ilenia Segatto<sup>1</sup>, Vincenzo Canzonieri<sup>2</sup>, Daniela Marconi<sup>3</sup>, Monica Schiappacassi<sup>1</sup>, Sara Benevol<sup>1</sup>, Valter Gattei<sup>3</sup>, Alfonso Colombatti<sup>1,4</sup>, Barbara Belletti<sup>1,\*</sup>, and Gustavo Baldassarre<sup>1,\*</sup>

<sup>1</sup>Department of Translational Research; Division of Experimental Oncology 2; CRO of Aviano, National Cancer Institute; Aviano, Italy; <sup>2</sup>Pathology Unit; CRO of Aviano; National Cancer Institute; Aviano, Italy; <sup>3</sup>Clinical and Experimental Onco-Hematology Unit; CRO of Aviano, National Cancer Institute; Aviano; Italy; <sup>4</sup>Department of Biomedical Sciences and Technologies; MATI Center of Excellence; University of Udine; Udine, Italy

<sup>†</sup>These authors contributed equally to this work and should be recognized as co-first authors.

**Keywords:** cell cycle, gene knock-out, p27<sup>kip1</sup>, proliferation, signaling pathway, stathmin

**Abbreviations:** CDK, cyclin-dependent kinase; WT, wild type; KO, knock-out; DKO, double knock-out; Stm, stathmin; BrdU, 5-bromo-2-deoxyuridine; JAK-STAT, janus kinase/signal transducers and activators of transcription; MAPK, mitogen-activated protein kinase.

The CDK inhibitor p27<sup>kip1</sup> is a critical regulator of cell cycle progression, but the mechanisms by which p27<sup>kip1</sup> controls cell proliferation in vivo are still not fully elucidated. We recently demonstrated that the microtubule destabilizing protein stathmin is a relevant p27<sup>kip1</sup> binding partner. To get more insights into the in vivo significance of this interaction, we generated p27<sup>kip1</sup> and stathmin double knock-out (DKO) mice. Interestingly, thorough characterization of DKO mice demonstrated that most of the phenotypes of p27<sup>kip1</sup> null mice linked to the hyper-proliferative behavior, such as the increased body and organ weight, the outgrowth of the retina basal layer and the development of pituitary adenomas, were reverted by co-ablation of stathmin. In vivo analyses showed a reduced proliferation rate in DKO compared to p27<sup>kip1</sup> null mice, linked, at molecular level, to decreased kinase activity of CDK4/6, rather than of CDK1 and CDK2. Gene expression profiling of mouse thymuses confirmed the phenotypes observed in vivo, showing that DKO clustered with WT more than with p27 knock-out tissue. Taken together, our results demonstrate that stathmin cooperates with p27<sup>kip1</sup> to control the early phase of G1 to S phase transition and that this function may be of particular relevance in the context of tumor progression.

## Introduction

The coordinated transmission of information from the outside to the inside of the cell, i.e. the signal transduction, represents a very delicate process for any living entity. For a balance to be achieved, the components of the signaling networks have to be precisely integrated in time and space.<sup>1,2</sup> Cell division is a typical example in which external signals from the local microenvironment are integrated with those present inside the cell before the final commitment to enter the cell cycle and divide is taken. The necessity of a tight regulation of this process is demonstrated by the fact that uncontrolled proliferation represents one and the most obvious hallmark of cancer.<sup>3</sup> External stimuli (e.g. growth factor stimulation, cell adhesion, etc) are required to pass through the restriction point and the activated intracellular signal

transduction pathways directly impinge on the cell cycle machinery, modulating the expression and/or the subcellular localization of 2 key regulators of the G1 to S phase transition, p27<sup>kip1</sup> and cyclin D1.<sup>4,5</sup>

The tumor suppressor protein p27<sup>kip1</sup> (hereafter p27) was originally identified as a cyclin/CDK inhibitor, in particular of the CDK2-containing complexes (for a review see refs. 6, 7). Subsequent studies demonstrated that it is also implicated in the regulation of several other biological activities, such as differentiation, apoptosis, motility and autophagy.<sup>6,7</sup>

Formal demonstration that p27 is a tumor suppressor gene and a fundamental negative regulator of cell cycle progression primarily arose from characterization of p27 knock-out mice.<sup>8-10</sup> Most prominent phenotypes of p27 null animals comprise increased body size (about 10-20% respect to the wild type littermates), pituitary adenoma formation, outgrowth of the retina

© Stefania Berton, Ilenia Pellizzari, Linda Fabris, Sara D'Andrea, Ilenia Segatto, Vincenzo Canzonieri, Daniela Marconi, Monica Schiappacassi, Sara Benevol, Valter Gattei, Alfonso Colombatti, Barbara Belletti, and Gustavo Baldassarre

\*Correspondence to: Gustavo Baldassarre; Email: gbalassarre@cro.it; Barbara Belletti; Email: bbelletti@cro.it

Submitted: 05/28/2014; Revised: 07/22/2014; Accepted: 07/24/2014

<http://dx.doi.org/10.4161/15384101.2014.949512>

This is an Open Access article distributed under the terms of the Creative Commons Attribution-Non-Commercial License (<http://creativecommons.org/licenses/by-nc/3.0/>), which permits unrestricted non-commercial use, distribution, and reproduction in any medium, provided the original work is properly cited. The moral rights of the named author(s) have been asserted.

basal layer and female infertility.<sup>8-10</sup> All these traits have been originally ascribed to the higher CDK2 activity and increased cell proliferation rate displayed by tissues.<sup>8-10</sup> However, subsequent generation of p27/CDK2 double knock-out mice demonstrated that these animals retained all major phenotypes of p27 null animals, thus excluding that CDK2 represented the major target of p27 inhibition and suggesting that other pathways were implicated.<sup>11,12</sup>

We recently demonstrated that the microtubules-destabilizing protein stathmin is a cytoplasmic binding partner of p27 and that this interaction plays a role in the control of cell motility.<sup>13-17</sup> No overt phenotype has been described to stathmin null mice,<sup>18-20</sup> except for behavioral defects linked to the control of learned and innate fear.<sup>21,22</sup> However, stathmin expression plays a pivotal role in cell cycle regulation and in cancer progression,<sup>23</sup> suggesting that it could influence both cell proliferation and migration, at least in some contexts.

To test this hypothesis, we used a genetic approach and analyzed whether stathmin is a relevant target of p27 *in vivo*.

Here, we report the generation and characterization of p27 and stathmin double knock-out mice. Surprisingly, stathmin deletion in p27 knock-out backgrounds reverts many of the proliferation-related phenotypes displayed by the p27 knock-out mouse. Our findings demonstrate that p27/stathmin interaction plays a pivotal role in the control of cell proliferation *in vivo* and suggest that this function might be particularly relevant in the process of tumor progression.

## Results

### Stathmin knock-out reverts the gigantism of p27 null mice

Our previous work highlighted a novel function of p27 in the control of motility and invasion. This function relied on p27 interaction with stathmin, with consequent modulation of microtubule dynamics.<sup>13-17</sup> To get more insights into the physiological role of p27/stathmin interaction, we generated p27/stathmin double knock-out (hereafter DKO) mice, in the C57BL/6 background. The analysis of genomic DNA by PCR, of total RNA by

qRT-PCR and of protein levels by Western Blot confirmed the absence of p27 and stathmin expression in all analyzed tissues of DKO mice (Fig. S1A-D and data not shown). Stathmin was expressed in all tested adult mouse organs, although at variable levels, with no significant difference between wild type (WT) and p27 knock-out mice (Fig. S1B-D).

The analyses of more than 600 animals of the combined genotypes demonstrated that DKO mice were born at a percentage lower than expected by a Mendelian ratio (Fig. S2). The reduction in the expected Mendelian ratio was confirmed by crossing mice of different genotype, although at variable extent (Fig. S2). In particular, by intercrossing p27 heterozygous with stathmin knock-out (StmKO) mice ( $p27^{+/-} Stm^{-/-} \times p27^{+/-} Stm^{-/-}$ ), we obtained 13.36% DKO alive mice versus the expected 25%, suggesting that half of the DKO mice did not survive (Fig. S2A). Similar results were obtained when the crossing between  $p27^{+/-} Stm^{+/-}$  females with  $p27^{-/-} Stm^{+/-}$  males was examined (Fig. S2B), while the percentage of observed DKO mice was even lower by crossing double heterozygous mice (Fig. S2C). Accordingly, analysis of the genotypes of embryos taken at day 13.5 of gestation demonstrated approximately a 50% reduction in DKO embryos observed respect to expected, in both C57BL/6 and FVB backgrounds (Fig. S2D). However, DKO embryos that eventually survived did not show any evident morphological defect (Fig. S2D). Overall, these analyses demonstrated that a genetic interaction between p27 and stathmin exists at organism level and that half of DKO embryos die before day 13.5. Further investigation will be needed to better address this issue and clarify this phenotype.

Next, we analyzed the growth of mice of the different genotypes during the first 14 weeks. This is the period in which p27KO animals display the greatest differences respect to their wild type (WT) littermates.<sup>8</sup> The comparative analysis of p27KO (n = 87), DKO (n = 77), WT (n = 57) and StmKO (n = 140) mice showed that the increased body size, peculiar of p27 null animals, was almost completely reverted in DKO mice (Figs. 1A and B). This was particularly evident in males, where WT (n = 27) and DKO (n = 41) weighed similarly and

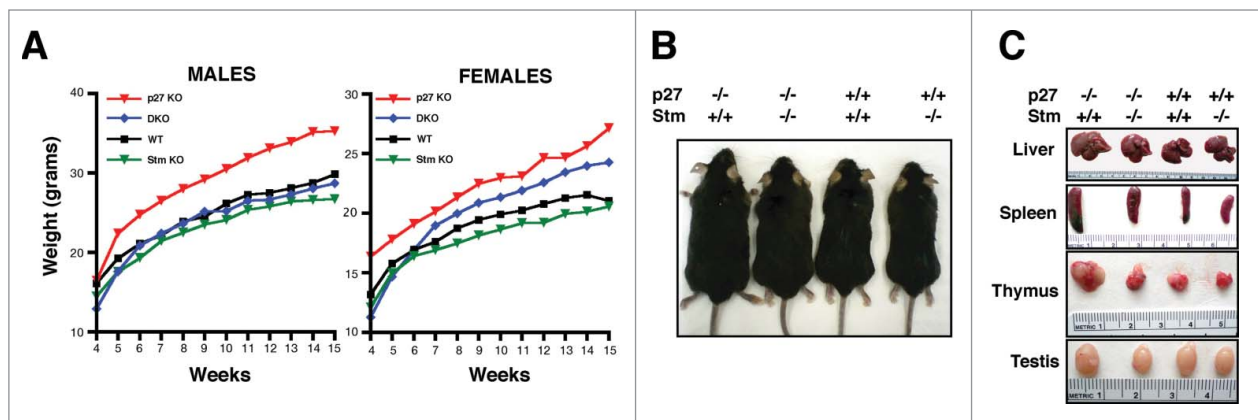


**Figure 1.** Stathmin loss reverts the gigantism of p27 null mice. **(A)** Growth curves of C57BL/6 mice WT (27 males, 30 females), p27KO (43 males, 44 females), DKO (41 males, 36 females) and StmKO (65 males, 75 females), weighed every week, from 4 to 15 weeks of age (p27KO vs WT and DKO,  $p < 0.01$ , at all time points considered). **(B and C)** Representative images of 15-week-old C57BL/6 mice and organs of the indicated genotypes.

significantly less than p27KO animals ( $n = 43$ ). StmKO male mice ( $n = 65$ ) did not significantly differ from WT and DKO animals in their growth (Fig. 1A, left panel and Fig. 1B), as reported also by others.<sup>18,19</sup> Among female animals more variability was observed. In this group, DKO ( $n = 36$ ) mice showed an intermediate phenotype between WT ( $n = 30$ ) and p27KO ( $n = 44$ ), while StmKO ( $n = 75$ ) weighed slightly less than WT and significantly less than DKO littermates (Fig. 1A, right panel). This evidence supports the possibility that p27 controls mice growth by different mechanisms including endocrine regulation, as already demonstrated for tumor development in p27 null animals.<sup>24</sup> In parallel, we performed accurate macroscopic observation of internal organs of mice sacrificed at specific times of their development. This analysis confirmed that p27 absence led to enlargement of all organs and, particularly, of lymphoid organs.<sup>8-10</sup> Also this phenotype was significantly reverted in DKO animals (Fig. 1C and D). To evaluate the possibility that the observed phenotypes could be strain-related, we moved the DKO C57BL/6 mice in different genetic backgrounds, by intercrossing WT FVB and WT 129S2/Sv with p27<sup>+/-</sup> Stm<sup>+/-</sup> C57BL/6 mice, until N6, to obtain near congenic FVB and 129S2/Sv colonies. The Strain GenCheck™ SNP Profiling on 5 different mice/strain confirmed the identity of each strain (Fig. S3A). Body weight analyses confirmed that, also in the FVB genetic background, DKO mice weighed similarly to the WT counterpart and significantly less than their p27KO littermates (Fig. S3B and C).

The effects of p27 loss on mouse body size is known to be gene-dosage dependent.<sup>8-10</sup> Thus we evaluated the possibility that also stathmin exerted a gene-dosage effect, *in vivo*. The analyses of more than 1000 mice of the different genotypes showed that, in the context of p27 heterozygous mice, the loss of stathmin reverted the increased body weight of p27<sup>+/-</sup> mice in a gene-dosage dependent manner (Fig. S4A–C). On the contrary, in the context of p27 null background, the loss of one single allele of stathmin (i.e., p27<sup>-/-</sup>Stm<sup>+/-</sup> mice) was not sufficient to reduce their increased body weight (Fig. S4D).

#### Stathmin knock-out reverts the organomegaly of p27 null mice

Since knock-out of p27 gene leads to particular enlargement of lymphoid organs,<sup>8-10</sup> we first focused our analyses on thymus and spleen. By calculating the ratio between organ/body weights of 15 weeks old mice, we observed a significant reduction in DKO mice when compared to p27KO animals (Fig. 2A). It has been demonstrated that the enlargement of p27KO lymphoid organs is due to higher cell number.<sup>8-10</sup> Accordingly, analyses of 10 weeks old males ( $n = 3$ /group) for weight and cell number in lymphoid organs indicated the presence of higher numbers of both splenocytes and thymocytes in p27KO respect to DKO and WT mice (Fig. 2B). The differences between p27KO and the other genotypes were particularly evident for thymocytes, which were highly and more significantly reduced in DKO animals (Fig. 2B). This observation prompted us to verify if the difference in organ weight directly correlated with the expression of

stathmin in adult organs. To this aim, we looked at the weights of the 3 organs in which stathmin was most highly expressed, namely the brain, the thymus and the testis, and of a organ displaying lower stathmin expression, such as the spleen (Figs. 1 and 2C). Interestingly, the levels of stathmin inversely correlated with organ weights (Fig. 2D). Organs expressing high levels of stathmin displayed a more evident and significant weight reduction in DKO mice respect to p27KO ones and not statistically significant differences between DKO, WT and StmKO mice were detected (Fig. 2D). Conversely, spleens, which express very low levels of stathmin, displayed an intermediate weight in DKO mice respect to p27KO and both WT and StmKO mice. These data were further confirmed in p27 heterozygous and knock out mice, in which stathmin biallelic deletion significantly reduced the weight of all analyzed organs, except for spleens (Fig. S5). These findings reinforce the hypothesis that, when abundantly expressed, stathmin participated with p27 to the control of mouse and organ growth.

Organomegaly in p27KO mice has been linked to increased proliferation rates.<sup>8-10</sup> Thus, we tested whether other 2 known phenotypes of p27KO mice linked to altered cell proliferation, the outgrowth of the retina basal layer and the development of pituitary adenomas, were also influenced by concomitant stathmin knock-out.

First, we analyzed retinas explanted from 5-8 weeks-old mice. As previously reported, we observed that all p27KO mice displayed outgrowth of the retina basal layer (Fig. 3A and B). In order to exclude possible artifacts due to samples fixing, processing and staining and to obtain a quantification of the outgrowth, we scored the cell groups (more than 10 cells) grown outside the retina basal layer, in  $n = 10$  p27KO mice (20 retinas) (Fig. 3A, arrows). Using this criterion we observed that, on average, p27KO mice presented 2.3 lesions/retina (Fig. 3B). The same analysis was then performed in retinas from mice of the other genotypes. WT and StmKO retinas did not display any lesion and, more interestingly, DKO mice ( $n = 6$  mice,  $n = 12$  retinas) displayed only 0.5 lesions/retina. Immunofluorescence analyses confirmed that stathmin was well expressed in the retina of WT and p27KO mice and that it was clearly visible in the cells grown outside of the basal layer (Fig. 3C, arrows).

Then, we analyzed the pituitary glands collected from 1-year-old mice. In accord with published data<sup>25</sup> we observed that 27% of one-year old C57BL/6 p27KO mice developed pituitary adenoma of the intermediate part (Fig. 4A). Immunofluorescence analyses showed that stathmin was expressed in adult pituitary gland of WT and p27KO mice (Fig. 4B) and that its expression increased in the hyperplastic intermediate part of the gland (Fig. 4B, see p27KO panels). Strikingly, we did not observe any adenoma in age-matched WT, stathmin KO and DKO mice, although an enlargement of the intermediate part of the pituitary glands was observed in the latter genotype (Fig. 4A and C). The analysis of 1-year-old p27KO mice heterozygous for stathmin (p27<sup>+/-</sup> Stm<sup>+/-</sup>) showed a reduction in the animals that developed pituitary adenomas (18%), accompanied by an evident, although not significant, decrease in the mean pituitary gland

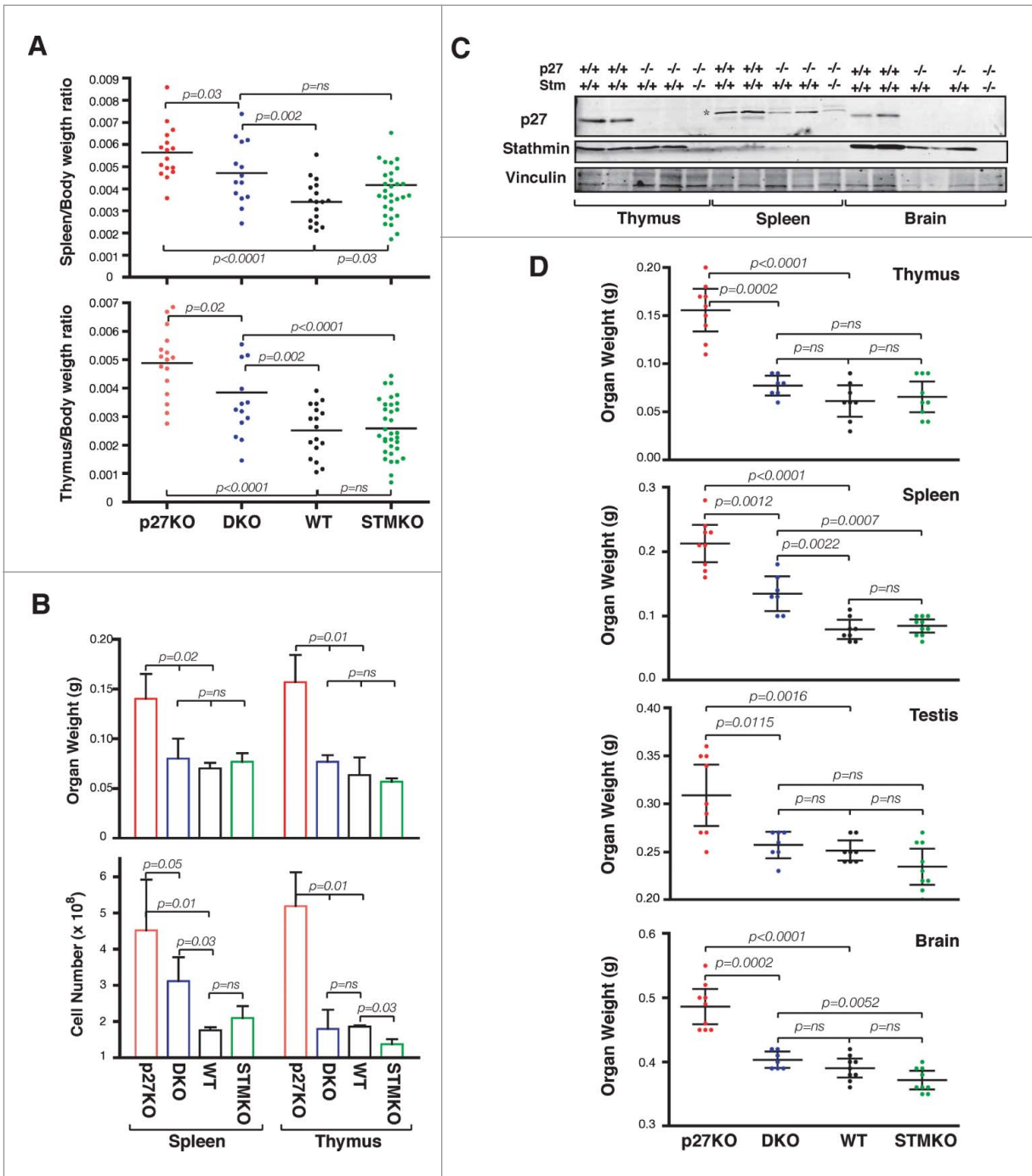


**Figure 2.** Stathmin loss reverts the increased organ size of p27KO mice. **(A)** Graphs report the organ/body ratio of spleens (upper panel) and thymuses (lower panel) from WT, p27KO, DKO and StmKO 15-week-old C57BL/6 mice. Each dot corresponds to one mouse. **(B)** Graphs report the weight (upper panel) and number of cells/organ (lower panel) in spleens and thymuses from WT, p27KO, DKO and StmKO 10-week-old C57BL/6 mice. **(C)** Western Blot analysis of p27 and stathmin expression in thymus, spleen and brain lysates, obtained from 2 WT, 2 p27KO and one DKO C57BL/6 mice, as indicated. Vinculin was used as loading control. Asterisk indicates non-specific bands detected by anti-p27 antibody. **(D)** Graphs report the weights of thymus, spleen, testis and brain from mice of the indicated genotypes. Each dot corresponds to one mouse. In each graph, statistical significance is calculated by unpaired t-test and expressed by a p value  $\leq 0.05$  (ns, not significant).

volume respect to that of p27 null animals (Fig. 4C). Since C57BL/6 mouse strain is particularly resistant to develop pituitary adenomas,<sup>25</sup> we also examined pituitary glands extracted from 5-9 months-old p27KO (n = 16) and DKO (n = 9) mice

of the 129S2/Sv background (Fig. 4D), which, conversely, is highly prone to develop pituitary adenomas.<sup>8,25</sup> As observed in the other genetic backgrounds (Fig. 1; Fig. S3), deletion of stathmin in p27 null background also reverted the increased body size

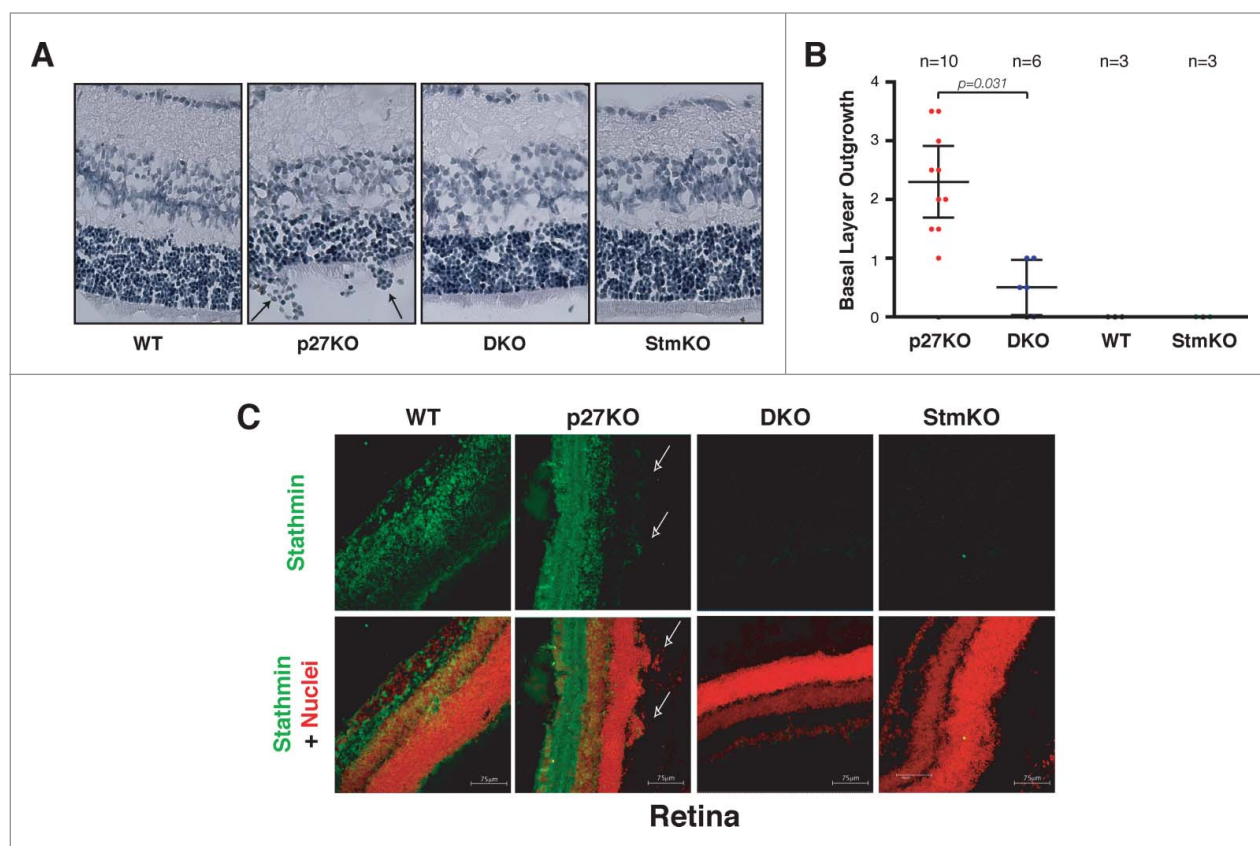


**Figure 3.** Stathmin loss reverts the outgrowth of the retina basal layer of p27KO mice. **(A)** H&E staining of the retina in sections from 5-weeks-old WT, p27KO, DKO and StmKO C57BL/6 mice. Black arrows indicate groups of cells outgrowing from the retina basal layer. **(B)** Graphs report the quantification of retina outgrowth in mice of the indicated genotypes. Only groups of 10 or more cells were counted. The number of analyzed mice is reported in the graph. Statistical significance is calculated by unpaired t-test and expressed by a p value  $\leq 0.05$ . **(C)** Confocal images of immunofluorescence analysis of stathmin (green) and nuclei (red) in retinal sections from WT, p27KO, DKO and StmKO C57BL/6 5-weeks-old mice. Bottom panels represent the merge of the 2 staining. Pictures show the endogenous expression of stathmin in murine retinas from WT and p27KO animals and its absence in tissue from DKO and StmKO mice, demonstrating the specificity of the immunostaining. Arrows indicate groups of stathmin positive cells outgrowing from the basal layer of the retina. A 40x objective was used.

phenotype (Fig. 4D). Moreover, analyses on the pituitary glands demonstrated that, while 94% of p27KO mice developed adenomas within 9 months of age (n = 15/16), only 55% of age-matched DKO animals developed the same pathology (n = 5/9) (Fig. 4E). However, in those 129S2/Sv DKO mice that did not develop an adenoma, we observed an enlargement of the intermediate part of the pituitary, as displayed by the C57BL/6 strain (Figs. 4A and C).

#### Stathmin is necessary for the hyper-proliferative phenotype of p27 null mice

We next asked whether proliferation was involved in the phenotypes observed above. Using the Ki67 antigen as marker of proliferating cells, we observed that the number of Ki67 positive cells (Ki67+) was significantly higher in p27KO respect to both WT and DKO pituitary glands (Figs. 5A and B), again suggesting that in vivo regulation of cell proliferation by p27 relayed, at least in part, on the expression of stathmin.

Next, we investigated the proliferation index of thymus, in which both p27 and stathmin are known to play a prominent role.

Using the Ki67 marker, we calculated the proliferation index in thymuses from 10-weeks-old mice. The proliferation index of DKO thymuses was significantly lower than the one observed in p27KO mice (Fig. 5C and D). Conversely, no significant difference was observed between WT, DKO and StmKO thymuses (Fig. 5C). In accord with these observations, using an in vivo BrdU incorporation assay we detected a significant increase of proliferating cells in tissues from p27KO mice respect to both WT and DKO ones (Fig. 5E and F). When the number of apoptotic cells was assayed by TUNEL assays on tissue specimens, we could not observe any difference between DKO and p27KO mice (Fig. 5G), reinforcing the concept that proliferation was the process primarily affected by stathmin knockout in the p27 null background.

#### p27 is a master regulator of CDK2 activity, independently from stathmin expression

The above data supported that p27 controls cell proliferation in vitro and in vivo, at least partially, via stathmin. Previous works suggested that increased proliferation rate observed in p27 null animals was linked to increased CDK2 and, to lesser extent,

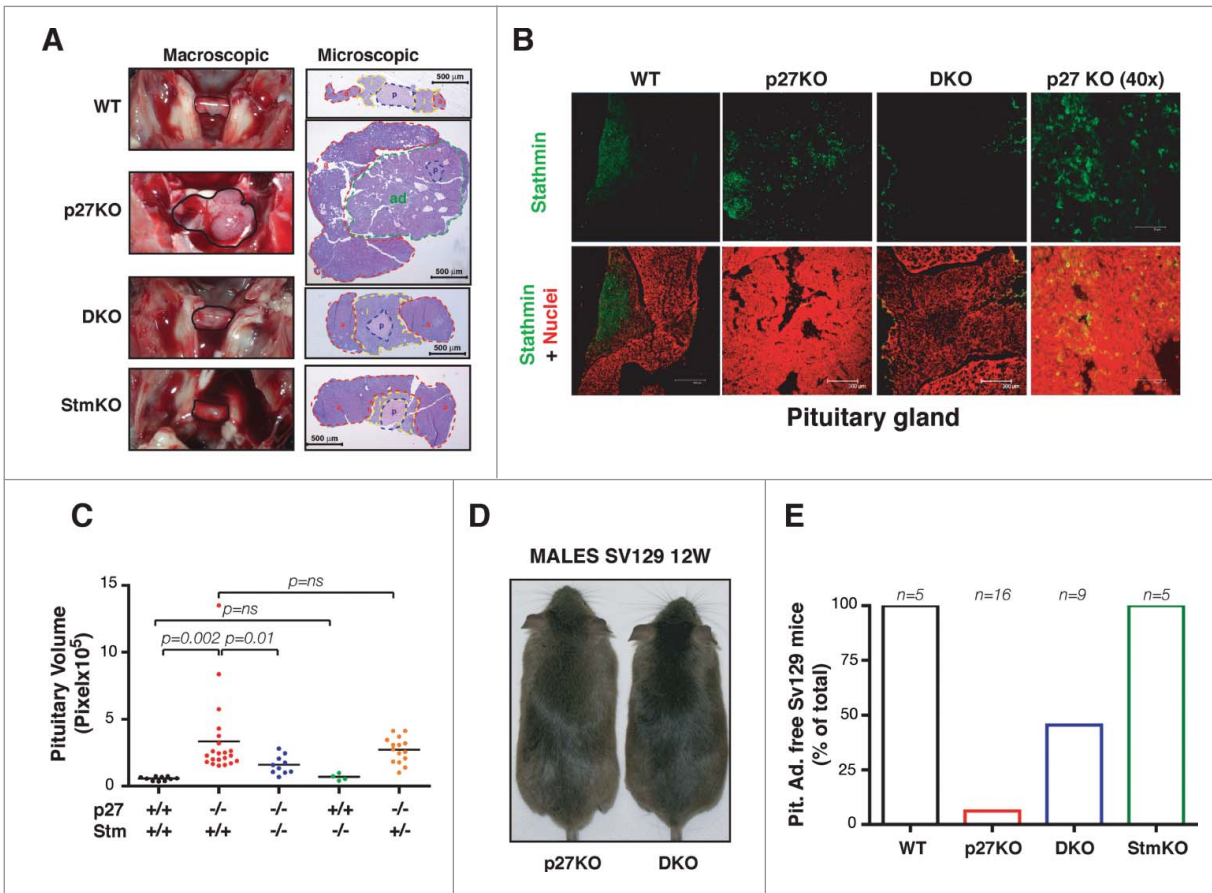


**Figure 4.** Stathmin loss suppresses the development of pituitary adenomas of p27KO mice. **(A)** Representative images of pituitary glands from 1-year-old C57BL/6 mice (outlined in black) of the indicated genotypes, photographed in situ (left panels, macroscopic) or H&E stained and captured with a 5x objective (right panels, microscopic). The pars posterior (p, in blue), the pars intermedia (i, yellow), the pars anterior (a, red) and the adenoma (ad, green) are outlined. **(B)** Confocal images of immunofluorescence analysis of stathmin (in green) and nuclei (in red) in pituitary gland sections from WT (10x), p27KO (10x and 40x) and DKO (10x) 1-year-old C57BL/6 mice. Bottom panels represent the merge of the 2 staining. **(C)** Graph shows pituitary gland volume of 1-year-old C57BL/6 mice of the different genotypes, as indicated. **(D)** Representative images of 12-weeks-old 129S2/Sv (SV129) male mice of the indicated genotypes. **(E)** Graph shows the number of 129S2/Sv (SV129) mice of the indicated genotypes (5-9 months old) that did not developed pituitary adenomas. The number of analyzed mice is reported in the graph.

CDK1 activity.<sup>8-12</sup> We thus wondered whether stathmin could impact on the activities of CDK2 and/or CDK1. As expected, CDK2- and CDK1-associated kinase activities were higher in p27KO respect to WT but, unexpectedly, not different between p27KO and DKO thymuses, both in the FVB (Fig. 6A) and the C57BL/6 (Fig. 6B) strains, in all the experiments performed. Since stathmin is a substrate of both CDK2 and CDK1,<sup>23,26,27</sup> we tested whether its expression could directly or indirectly influence their kinase activity. To test this possibility, increasing doses of recombinant stathmin protein were added to CDK2-containing complexes and their kinase activity was evaluated. The presence of stathmin did not significantly change the activity of CDK2 (Fig. 6C). Moreover, recombinant stathmin did not alter the kinase activity of cyclin A2/CDK2 recombinant complexes, neither it significantly overcame the block imposed by p27 on cyclin A2/CDK2 activity (Fig. 6D). Overall, these data confirmed that p27 is a master regulator of CDK2 activity, both in vitro and in vivo and further highlighted that the higher CDK2 activity observed in p27 null cells and organs is not sufficient to

explain their increased proliferation rate, as previously reported also by other groups.<sup>11,12</sup>

We next examined the activity of CDK4-, CDK6- and cyclin D3-complexes, which are primarily involved in the progression from early to late G1, in thymocytes<sup>28</sup> (Fig. 6) and splenocytes (Fig. S6). We could detect that the absence of p27 invariably resulted in a stathmin-dependent increased activity of CDK4, CDK6 and cyclin D3 complexes, as demonstrated by their decreased activity in DKO compared to p27KO thymuses and spleens (Figs. 6A and B; Fig. S6B). These results, coupled with the cell cycle analyses performed in splenocytes and thymocytes (Fig. S6A and data not shown) suggested that the increased proliferation of p27KO mice relies, at least in part, on the expression of stathmin that is, in turn, necessary to sustain CDK4/6 activity.

#### p27/stathmin interaction regulates gene expression in mouse thymus

To identify pathways potentially implicated in the establishment of the above described phenotypes, we performed a

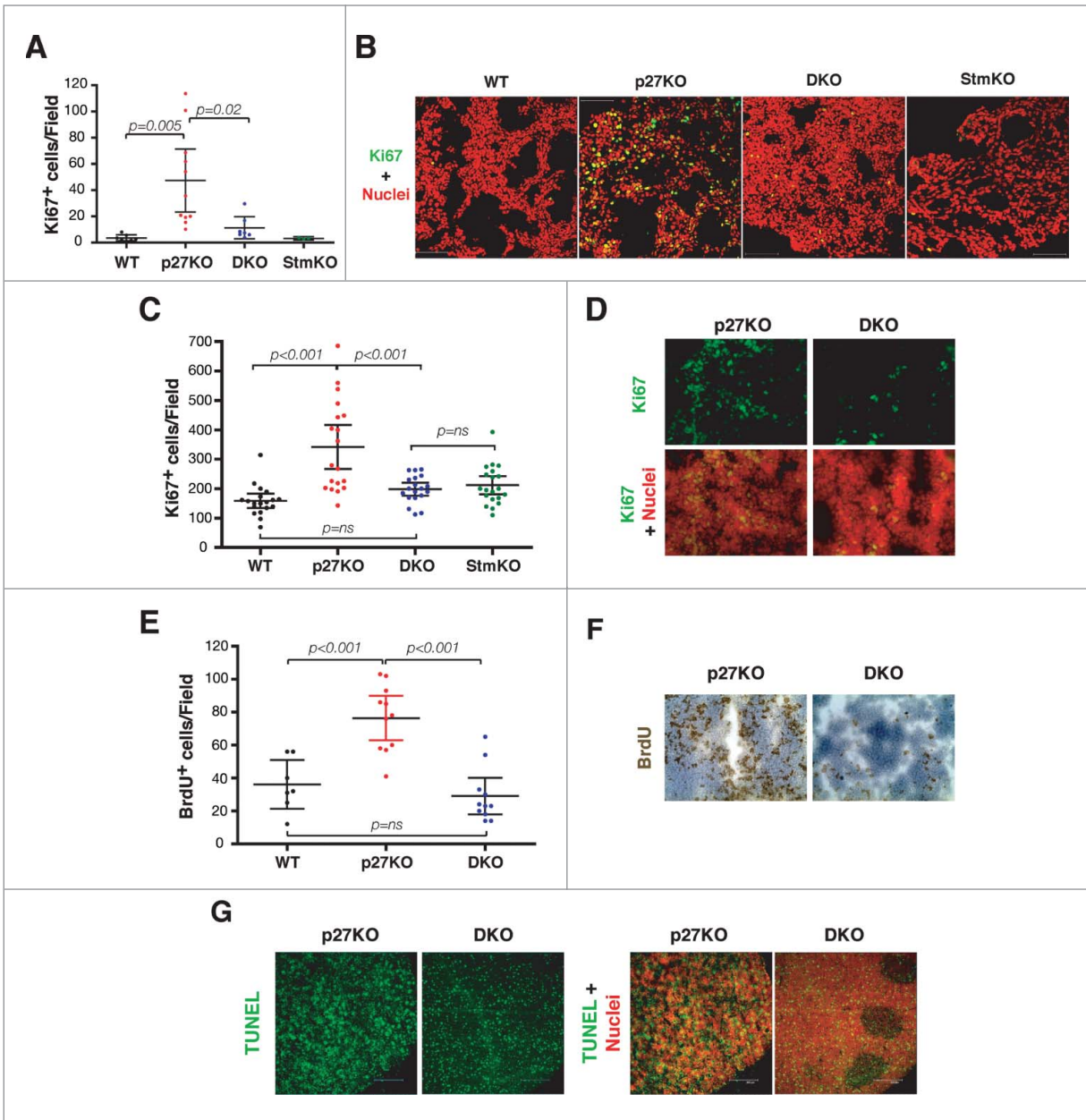


**Figure 5.** Stathmin is necessary for the hyper-proliferative phenotype of p27 null mouse organs. **(A)** Graph reports Ki67 positive cells in pituitary glands from 1-year-old C57BL/6 mice of the indicated genotypes. **(B)** Confocal images of immunofluorescence analysis of Ki67 (in green) and nuclei (in red) in pituitary gland sections from WT, p27KO, DKO and StmKO 1-year-old C57BL/6 mice, using a 40x objective. **(C)** Plot reports Ki67 positive cells in thymuses from 10-weeks-old C57BL/6 mice of the indicated genotypes. **(D)** Confocal images of immunofluorescence analysis of Ki67 (in green) and nuclei (in red) in thymus sections from p27KO and DKO (10x objective) 10-weeks-old C57BL/6 mice. Bottom panels represent the merge of the 2 staining. **(E)** Graph reports BrdU positive cells in thymuses from 20-weeks-old FVB mice of the indicated genotypes. **(F)** Typical images of immunohistochemistry analysis of BrdU expression in thymus sections from p27KO and DKO mice. **(G)** Confocal images of immunofluorescence analysis of TUNEL positive (in green) and nuclei (in red) in thymus sections from p27KO and DKO (10x objective) 10-weeks-old C57BL/6 mice. Left panels represent the merge of the 2 staining.

microarray analysis on thymuses collected from WT, p27KO, DKO and StmKO mice (3 males and 3 females, for each genotype). By comparing the gene expression profiles of WT and p27KO thymuses, we underscored a p27-signature, comprising 34 differentially regulated genes (Fig. 7). By comparing the gene expression profiles of WT and StmKO thymuses, we underscored

a stathmin-signature, comprising 69 differentially regulated genes (Fig. S7). We next made a comparative analysis of the DKO profile respect to the 2 signatures. When analyzed respect to the p27-signature, DKO clustered with WT rather than with p27KO profile, confirming, at gene expression level, what we observed at phenotypic level (Fig. 7). When analyzed respect to

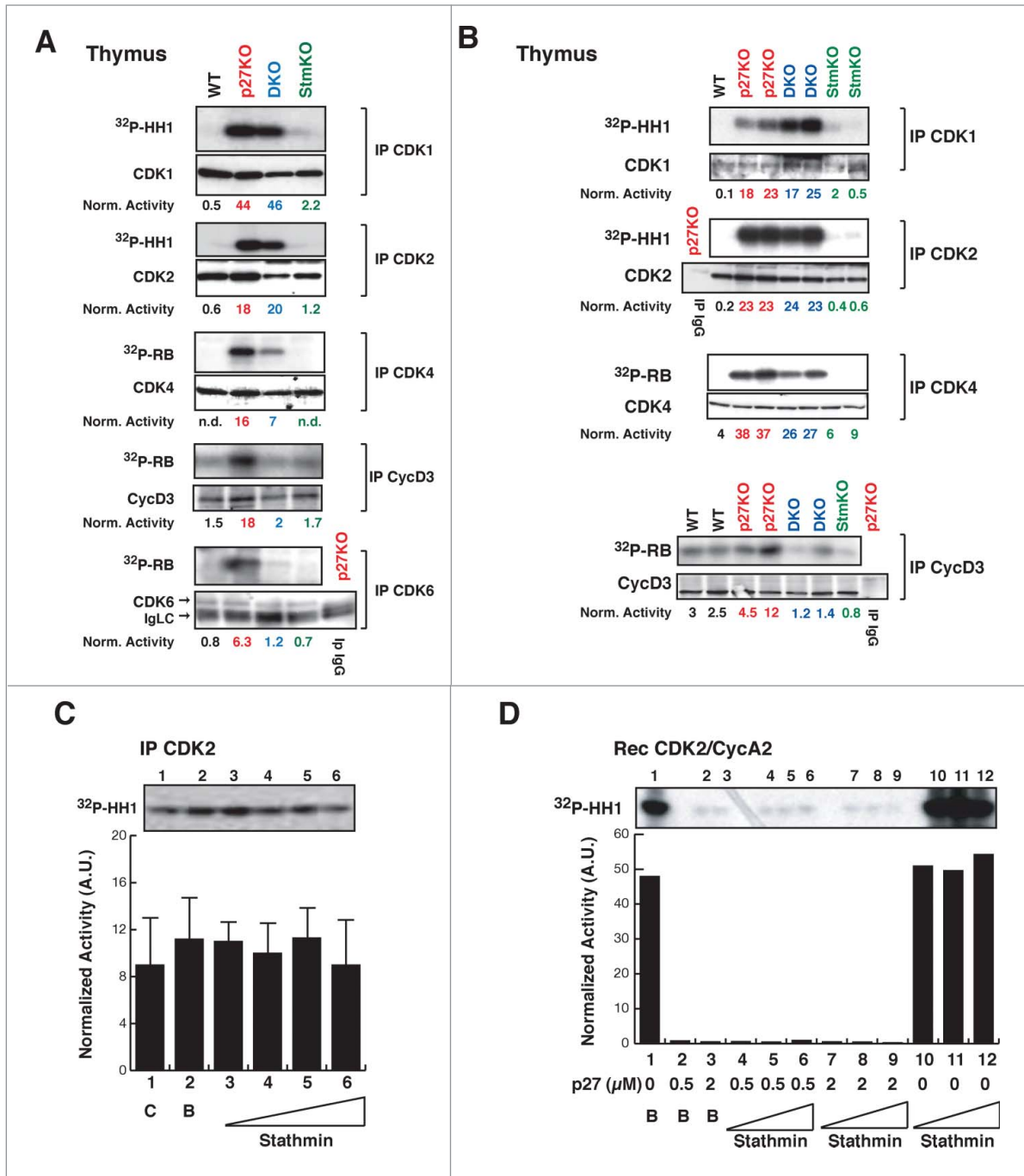


**Figure 6.** CDK4/6 activity is decreased in thymus from DKO mice. (A-B) Kinase activity (using <sup>32</sup>P-HH1 or <sup>32</sup>P-RB as substrates, as indicated) associated with the indicated immunoprecipitated (IP) proteins, from thymuses of WT, p27KO, DKO and StmKO FVB (A) and C57BL/6 (B) mice. Numbers at the bottom of the panels indicate the kinase activity normalized for the associated IP protein. (C) Kinase activity associated with the indicated immunoprecipitated (IP) proteins from lysates of exponentially growing SCC9 head and neck carcinoma cells, using histone H1 as substrate (<sup>32</sup>P-HH1). Lane 1 is the IP (C), lane 2 is the IP with imidazole (B), lanes from 3 to 6 are IPs incubated with increasing doses of recombinant stathmin (0.25-0.5-1-2 μg), prior to immunoprecipitation. Values in the graphs represent the mean of 3 independent experiments ± SD. Differences in kinase activity in the presence of stathmin are not statistically significant. On top of the graph, the kinase activity observed in a typical experiment is shown. (D) Kinase activity associated with recombinant CDK2/CycA2 complex, using histone H1 (<sup>32</sup>P-HH1) as substrate, in the presence of recombinant p27 (0-0.5-2 μg) without or with increasing doses of stathmin (0-0.65-1.3-2.6 μg). On top of the graph, the kinase activity is shown.

the stathmin-signature, DKO clustered with StmKO more than with WT profile (Fig. S7). Altogether, these data indicated that some of the features of p27KO animals rely on the expression of stathmin, while only few of the features of StmKO animals seems to rely on the expression of p27.

Finally, using the Pathway Express online resource (<http://vortex.cs.wayne.edu/projects.htm>) we pursued the identification of specific pathways differentially expressed among p27WT, p27KO, DKO backgrounds that could explain the observed phenotypes. Results from this type of analysis showed that the p27-signature principally impacted on 3 pathways, namely “Graft vs. Host disease”, “Natural Killer mediated cytotoxicity” and “ErbB signaling pathway”, while the stathmin-signature mostly impacted on “JAK-STAT signaling pathway”, “Complement and coagulation cascade” and “MAPK signaling pathway”, overall indicating that p27/stathmin interaction could impinge on intracellular signal transduction pathways, thus eventually modifying cell cycle progression (Table 1). Accordingly, when

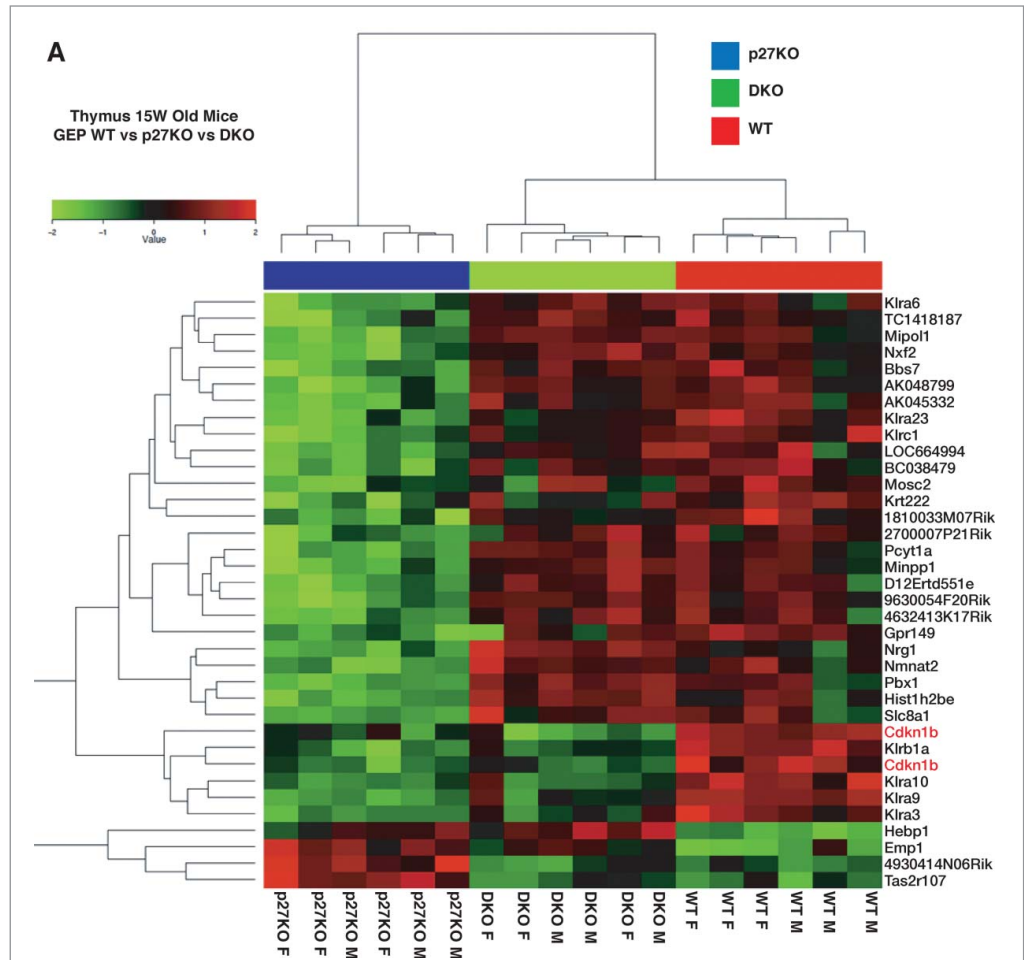


**Figure 7.** Gene expression profiling of WT, p27KO and DKO thymuses identifies a p27KO signature reverted in DKO mice. (A) Gene microarray analysis of RNA extracted from thymus of C57BL/6 mice of the indicated genotypes. Six different WT and p27KO thymuses/genotype (3 males and 3 females) were probed on a 44K microarray slides to identify genes differentially expressed in WT versus p27KO thymus (p27KO signature). The p27KO signature was then compared to the gene expression profile of DKO thymus (3 males and 3 females). This comparison identified the DKO signature, representing the set of genes differentially regulated between WT and p27KO cells and reverted in DKO thymus.

**Table 1.** Pathways altered in p27KO (p27 signature) and StmKO (stathmin signature) thymuses as evidenced using the online tools pathway express<sup>36</sup>

| Rank               | Pathway                              | I. F.  | Adj. p    |
|--------------------|--------------------------------------|--------|-----------|
| p27 Signature      |                                      |        |           |
| 1                  | Graft vs. Host disease               | 10.059 | 4.733 E-4 |
| 2                  | Natural Killer mediated cytotoxicity | 6.824  | 8.508 E-3 |
| 3                  | ERBB signaling pathway               | 4.335  | 6.990 E-2 |
| Stathmin Signature |                                      |        |           |
| 1                  | Jak-Stat signaling pathway           | 4.144  | 8,153 E-2 |
| 2                  | Complement and coagulation cascade   | 3.750  | 1,117 E-1 |
| 3                  | MAPK signaling pathway               | 2.548  | 2,776 E-1 |

I.F. = Impact factor  
Adj. p = Adjusted p value

we separately analyzed the gene expression profile of thymuses from male mice (n = 3/genotype), which displayed more significant differences in their phenotypes respect to females, we could observe that 264 genes were differentially expressed between WT and p27KO animals (Table S1) and, among the 4 GeneOntology (GO) processes most significantly different, actually 3 of them dealt with the regulation of signal transduction from the outside to the inside of the cell (Table 2; Table S2).

## Discussion

Here, we report the characterization of mice double knock-out (DKO) for p27 and stathmin genes. DKO mice display normal body weight and organ size, absence or low incidence of pituitary adenomas (depending on the mouse strain) and normal retina development, demonstrating that co-ablation of stathmin rescues most of the phenotypes observed in p27KO mice. At

**Table 2.** Pathways altered in p27KO (p27 signature) male thymuses as evidenced using the Gene Annotation Tool

| Rank                  | Pathway                                   | G.O.       | p value |
|-----------------------|---|------------|---------|
| p27 Signature (males) |   |            |         |
| 1                     | Detection of external stimulus            | GO:0009581 | < 0.001 |
| 2                     | Sensory perception                        | GO:0007600 | < 0.001 |
| 3                     | Response to stimulus                      | GO:0050896 | < 0.001 |
| 4                     | G-protein coupled receptor protein signal | GO:0007186 | < 0.001 |

G.O. = Gene Ontology number

molecular level, we show that decreased cell proliferation in DKO tissues was accompanied by a reduction in the activity of CDK4 and CDK6 containing complexes rather than to decreased activity of CDK2.

The observation that CDK2 knock-out was not able to rescue the phenotype of p27 null mice indirectly supports our work.<sup>11,12</sup> Indeed, p27 inhibits cell cycle progression even in cells that lack CDK2, suggesting that either CDK2 is not the primary target of p27 *in vivo*, or, alternatively, that p27 can block cell cycle progression by interacting with molecules other than CDK2, as we show here.<sup>12</sup> Assuming that one or more compensatory mechanisms exist, the most likely molecules that could compensate CDK2 loss would certainly be other CDKs involved in cell cycle progression, mainly CDK1, CDK4, and CDK6. The higher CDK1 activity observed in p27/CDK2 KO mice has been proposed as the principal compensatory mechanism, at least in that context.<sup>11</sup> However, in p27KO and DKO animals CDK1 activity is equally high, both in thymuses and spleens, suggesting that it is not primarily implicated in the phenotype observed in DKO animals. Conversely, we found that CDK4 and CDK6 were more active in p27KO respect to DKO lymphoid organs, suggesting that stathmin represents a critical determinant in the generation of lymphoid hyperplasia by governing CDK4/6 activity. These data are also in agreement with the observation made by Fero and collaborators,<sup>29</sup> showing that thymus hyperplasia of p27KO mice represents a non cell autonomous function of p27, probably relying on higher CDK4 activity present in the thymic epithelium.<sup>29</sup>

Our data also suggest that stathmin is necessary for the development of pituitary adenomas in p27 null mice. A careful observation of p27KO and DKO pituitary glands in the different genetic backgrounds that we analyzed, suggested that stathmin absence did not impair the development of hyperplasia of the pituitary intermediate pars, but rather impinged on the appearance of a frank pituitary adenoma. Thus, in the pituitary context, stathmin seems to be more relevant in the control of later steps of tumorigenesis rather than the initial ones. This observation is in agreement with our recent studies, showing that stathmin is dispensable for tumor onset in mice in several mouse models of carcinogenesis<sup>20</sup> and with the well established notion that stathmin is overexpressed in advanced tumors but not in early neoplastic lesions.<sup>23</sup>

The different proliferation index displayed by thymuses and pituitary glands of DKO animals respect to the p27KO but also to the WT ones, could be linked to the fact that p27 regulates *in vivo* growth by both cell autonomous and non cell autonomous mechanisms, depending on the tissue type.<sup>29</sup> This possibility is also supported by the observation of mice double knockout for p27 and cyclin D1.<sup>30,31</sup> Thymus hyperplasia is still present in cyclin D1/p27KO mice,<sup>31</sup> most likely because proliferation in the thymus primarily relies on cyclin D3 and CDK6, rather than cyclin D1 and CDK4.<sup>28,32,33</sup> On the other side, body weight and retinal dysplasia were both rescued in the cyclin D1/p27KO mice,<sup>30</sup> again highlighting how sophisticated the regulation of cell proliferation is in complex organisms.

Several data demonstrate that stathmin plays a pivotal role during mitosis, by regulating the assembly and disassembly of the mitotic spindle.<sup>23</sup> However, *in vivo* evidence showing a direct role of stathmin during mitosis essentially lacks. Our data propose an *in vivo* role for stathmin in the control of early G1 phase, by modifying CDK4 and CDK6 activity in the absence of p27. Since CDK4 and CDK6 are primarily involved in the control of G1 to S phase transition, our findings add a new layer of complexity to the role of stathmin in governing cell proliferation. Regulation of CDK4 and CDK6 activity and of cell proliferation by stathmin is evident only in the absence of p27. It is possible that, since p27 blocks stathmin activity,<sup>13,16</sup> the absence of p27 unmasks previously not appreciated functions of stathmin. This, in turn, could be particularly evident when stathmin expression is particularly high, such as in the hyperplastic pituitary gland and in brain, thymus and testis.

The phenotype of DKO animals is also reminiscent of the one recently described for miR-9 knock-down in neuronal stem cells.<sup>34</sup> In this model, miR-9 knock-down results in increased stathmin expression that eventually regulates cell proliferation. Interestingly, stathmin silencing reduced the hyper proliferation of miR-9 knock-down cells but was ineffective in cells still expressing miR-9,<sup>34</sup> again suggesting that stathmin participates in the control of cell proliferation especially when its expression/activity is particularly high, as in the case of p27 null animals. To better understand how increased stathmin activity could contribute to the regulation of cell proliferation, impinging on CDK4/6 activities in p27KO mice, we used a gene expression profile approach. Biological processes and signaling pathways involved in the response to and the transduction of external stimuli were more significantly different between p27KO and WT or DKO thymuses. This observation suggests that p27/stathmin interaction might, at least in tissues that express high levels of stathmin such as thymuses, impinge on the regulation of cell proliferation by altering the response to external stimuli, ultimately determining increased CDK4/6 activity. This possibility is in line with our recent observation that regulation of microtubule dynamics by p27/stathmin interaction governs cell motility acting on intracellular vesicular transport and Rho GTPases activity.<sup>16</sup> Thus, it is possible that p27/stathmin interaction could regulate cell proliferation by acting on key signal transduction players, like tyrosin kinase receptors or small GTPases, that are precisely activated in time and space

by intracellular transport and through vesicle recycling.<sup>35</sup> The investigation of the mechanisms by which CDK4 and CDK6 activity is regulated by stathmin, possibly via an altered intracellular signaling, as suggested by our data, represents an interesting field that certainly merits further investigation in the future.

In conclusion, this work identifies a new layer of complexity existing in the regulation of cell proliferation *in vivo* and opens several new questions regarding the role of cyclin/CDKs binding to p27 in the control of cell proliferation *in vivo*. Understanding whether the new regulatory axis here reported might play a role in cell transformation and how it might be tackled to counteract tumor progression, is certainly a field that deserves further investigation.

## Materials and Methods

Detailed description of methods used in this work may be found in the Supplemental Material section, available online.

All animal experiments were reviewed and approved by the CRO Institutional Animal Care and Use Committee and were conducted according to that committee's guidelines.

### Mice models and phenotypic characterization

Mice were maintained in CRO of Aviano animal facility, at 22°C with 40-60% of humidity. C57BL/6 p27 knock-out (p27KO) mice (The Jackson Laboratory) and C57BL/6 StmKO mice,<sup>18,20</sup> were intercrossed to obtain p27 and stathmin double KO (DKO) C57BL/6 mice. WT FVB (Charles River) and WT 129S2/Sv (Charles River) mice were crossed with p27+/- stathmin+/- C57BL/6 mice until N6, to obtain near congenic FVB and 129S2/Sv strains.

### Proliferation and apoptosis assays

Analysis of cell proliferation by BrdU incorporation assay, Ki67 staining and detection of apoptosis by TUNEL assay, are techniques routinely performed in our lab,<sup>13-17</sup> and better described in the Supplemental Material available online.

### Preparation of protein lysates, immunoprecipitation, immunoblotting and kinase assay

To extract proteins from mouse organs, tissue disruption was performed using the TissueLyser II (QIAGEN). Minced tissues were incubated in ice once dissolved in NP40 lysis buffer (0.5% NP40; 50 mM HEPES pH 7; 250 mM NaCl; 5 mM EDTA; 0.5 mM EGTA, pH 8) supplemented with protease inhibitor cocktail (Complete™, Roche), 1 mM Na<sub>3</sub>VO<sub>4</sub> (Sigma),

10 mM NaF (Sigma) and 1 mM DTT (Sigma). Immunoprecipitation (IP) experiments were performed using 0.5–1 mg of total lysate in HNTG buffer (20 mM HEPES, 150 mM NaCl, 10% Glycerol, 0.1% Triton X-100, protease inhibitor cocktail, 1 mM Na<sub>3</sub>VO<sub>4</sub>, 10 mM NaF and 1 mM DTT) with the specific agarose-conjugated primary antibodies. Immunoblotting was performed as previously described<sup>15,17</sup> and, following incubation with primary antibodies overnight at 4°C, incubated 1 hour at RT with IR-conjugated (Alexa Fluor 680, Invitrogen or IRDye 800, Rockland) secondary antibodies for subsequent infrared detection (Odyssey Infrared Detection System, Licor). Primary antibodies p27kip1 (C-19 and N-20), CDK2, CDK4, CDK6, cyclin D3 and Vinculin were purchased from Santa Cruz; CDK1 and p27Kip1 were purchased from BD; Stathmin was purchased from Sigma. Kinase assays were performed in kinase buffer (20 mM TrisHCl pH 6.8, 10 mM MgCl<sub>2</sub>) using, 1 μCi γ-P32 ATP and 2 μg of H1-Histone (Upstate Biotechnology) or recombinant pRB as substrate, as described.<sup>15,17</sup>

### Statistical analysis

Data were examined using the 2-tailed Student t test or unpaired 2-tailed Mann-Whitney U test. Differences were considered significant at *P* < 0.05. Computational analyses were performed according to Draghici et al.<sup>36</sup> All graph and statistical analyses were performed using GraphPad PRISM version 4.00.

### Disclosure of Potential Conflicts of Interest

No potential conflicts of interest were disclosed.

### Acknowledgments

We thank Dr. Joshua Armenia for pathways analysis and all members of the S.C.I.C.C. lab for their support and for helpful scientific discussions. We thank Dr. Riccardo Bomben of the Microarray facility, for useful suggestions and expert assistance.

### Funding

This work was supported by Associazione Italiana Ricerca sul Cancro (AIRC) to G.B. (IG 12854), by Ministry of Health (RF-2010–2309704) to G.B. and by CRO Intramural research grant to G.B.

### Supplemental Materials

Supplemental data for this article can be accessed on the publisher's website.

## References

1. Scott JD, Pawson T. Cell signaling in space and time: where proteins come together and when they're apart. *Science* 2009; 326:1220-4; PMID:19965465; <http://dx.doi.org/10.1126/science.1175668>
2. Good MC, Zalatan JG, Lim WA. Scaffold proteins: hubs for controlling the flow of cellular information. *Science* 2011; 332:680-6; PMID:21551057; <http://dx.doi.org/10.1126/science.1198701>
3. Hanahan D, Weinberg RA. Hallmarks of cancer: the next generation. *Cell* 2011; 144:646-74; PMID:21376230; <http://dx.doi.org/10.1016/j.cell.2011.02.013>
4. Vidal A, Koff A. Cell-cycle inhibitors: three families united by a common cause. *Gene* 2000; 247:1-15; PMID:10773440; [http://dx.doi.org/10.1016/S0378-1119\(00\)00092-5](http://dx.doi.org/10.1016/S0378-1119(00)00092-5)
5. Zwang Y, Sas-Chen A, Drier Y, Shay T, Avraham R, Lauriola M, Shema E, Lidor-Nili E, Jacob-Hirsch J, Amariglio N, et al. Two phases of mitogenic signaling unveil roles for p53 and EGR1 in elimination of inconsistent growth signals. *Mol Cell* 2011; 42:524-35; PMID:21596316; <http://dx.doi.org/10.1016/j.molcel.2011.04.017>
6. Belletti B, Nicoloso MS, Schiappacassi M, Chimienti E, Berton S, Lovat F, Colombatti A, Baldassarre G. p27(kip1) functional regulation in human cancer: a potential target for therapeutic designs. *Curr Med*

- Chem 2005; 12:1589-605; PMID:16022660; <http://dx.doi.org/10.2174/0929867054367149>
7. Chu IM, Hengst L, Slingerland JM. The Cdk inhibitor p27 in human cancer: prognostic potential and relevance to anticancer therapy. *Nat Rev Cancer* 2008; 8:253-67; PMID:18354415; <http://dx.doi.org/10.1038/nrc2347>
  8. Fero ML, Rivkin M, Tasch M, Porter P, Carow CE, Firpo E, Polyak K, Tsai LH, Broudy V, Perlmutter RM, et al. A syndrome of multiorgan hyperplasia with features of gigantism, tumorigenesis, and female sterility in p27(Kip1)-deficient mice. *Cell* 1996; 85:733-44; PMID:8646781; [http://dx.doi.org/10.1016/S0092-8674\(00\)81239-8](http://dx.doi.org/10.1016/S0092-8674(00)81239-8)
  9. Nakayama K, Ishida N, Shirane M, Inomata A, Inoue T, Shishido N, Horii I, Loh DY, Nakayama K. Mice lacking p27(Kip1) display increased body size, multiple organ hyperplasia, retinal dysplasia, and pituitary tumors. *Cell* 1996; 85:707-20; PMID:8646779; [http://dx.doi.org/10.1016/S0092-8674\(00\)81237-4](http://dx.doi.org/10.1016/S0092-8674(00)81237-4)
  10. Kiyokawa H, Kineman RD, Manova-Todorova KO, Soares VC, Hoffman ES, Ono M, Khanam D, Hayday AC, Frohman LA, Koff A. Enhanced growth of mice lacking the cyclin-dependent kinase inhibitor function of p27(Kip1). *Cell* 1996; 85:721-32; PMID:8646780; [http://dx.doi.org/10.1016/S0092-8674\(00\)81238-6](http://dx.doi.org/10.1016/S0092-8674(00)81238-6)
  11. Aleem E, Kiyokawa H, Kaldis P. Cdc2-cyclin E complexes regulate the G1/S phase transition. *Nat Cell Biol* 2005; 7:831-6; PMID:16007079; <http://dx.doi.org/10.1016/j.ncb1284>
  12. Martín A, Odajima J, Hunt SL, Dubus P, Ortega S, Malumbres M, Barbacid M. Cdk2 is dispensable for cell cycle inhibition and tumor suppression mediated by p27(Kip1) and p21(Cip1). *Cancer Cell* 2005; 7:591-8; PMID:15950907; <http://dx.doi.org/10.1016/j.ccr.2005.05.006>
  13. Baldassarre G, Belletti B, Nicoloso MS, Schiappacassi M, Vecchione A, Spessotto P, Morrione A, Canzonieri V, Colombatti A. p27(Kip1)-stathmin interaction influences sarcoma cell migration and invasion. *Cancer Cell* 2005; 7:51-63; PMID:15652749; <http://dx.doi.org/10.1016/j.ccr.2004.11.025>
  14. Schiappacassi M, Lovat F, Canzonieri V, Belletti B, Berton S, Di Stefano D, Vecchione A, Colombatti A, Baldassarre G. p27Kip1 expression inhibits glioblastoma growth, invasion, and tumor-induced neoangiogenesis. *Mol Cancer Ther* 2008; 7:1164-75; PMID:18483304; <http://dx.doi.org/10.1158/1535-7163.MCT-07-2154>
  15. Berton S, Belletti B, Wolf K, Canzonieri V, Lovat F, Vecchione A, Colombatti A, Friedl P, Baldassarre G. The tumor suppressor functions of p27(kip1) include control of the mesenchymal/amoeboid transition. *Mol Cell Biol* 2009; 29:5031-45; PMID:19596789; <http://dx.doi.org/10.1128/MCB.00144-09>
  16. Belletti B, Pellizzari I, Berton S, Fabris L, Wolf K, Lovat F, Schiappacassi M, D'Andrea S, Nicoloso MS, Lovisa S, et al. p27kip1 controls cell morphology and motility by regulating microtubule-dependent lipid raft recycling. *Mol Cell Biol* 2010; 30:2229-40; PMID:20194624; <http://dx.doi.org/10.1128/MCB.00723-09>
  17. Schiappacassi M, Lovisa S, Lovat F, Fabris L, Colombatti A, Belletti B, Baldassarre G. Role of T198 modification in the regulation of p27(Kip1) protein stability and function. *PLoS One* 2011; 6:e17673; <http://dx.doi.org/10.1371/journal.pone.0017673>
  18. Schubart UK, Yu J, Amat JA, Wang Z, Hoffmann MK, Edelmann W. Normal development of mice lacking metablastin (P19), a phosphoprotein implicated in cell cycle regulation. *J Biol Chem* 1996; 271:14062-6; PMID:8662897; <http://dx.doi.org/10.1074/jbc.271.24.14062>
  19. Liedtke W, Leman EE, Fyffe REW, Raine CS, Schubart UK. Stathmin-deficient mice develop an age-dependent axonopathy of the central and peripheral nervous systems. *Am J Pathol* 2002; 160:469-80; PMID:11839567; [http://dx.doi.org/10.1016/S0002-9440\(10\)64866-3](http://dx.doi.org/10.1016/S0002-9440(10)64866-3)
  20. D'Andrea S, Berton S, Segatto I, Fabris L, Canzonieri V, Colombatti A, Vecchione A, Belletti B, Baldassarre G. Stathmin is dispensable for tumor onset in mice. *PLoS One* 2012; 7:e45561; <http://dx.doi.org/10.1371/journal.pone.0045561>
  21. Shumyatsky GP, Malleret G, Shin R-M, Takizawa S, Tully K, Tsvetkov E, Zakharenko SS, Joseph J, Vronskaya S, Yin D, et al. stathmin, a gene enriched in the amygdala, controls both learned and innate fear. *Cell* 2005; 123:697-709; PMID:16286011; <http://dx.doi.org/10.1016/j.cell.2005.08.038>
  22. Martel G, Nishi A, Shumyatsky GP. Stathmin reveals dissociable roles of the basolateral amygdala in parental and social behaviors. *Proc Natl Acad Sci U S A* 2008; 105:14620-5; PMID:18794533; <http://dx.doi.org/10.1073/pnas.0807507105>
  23. Belletti B, Baldassarre G. Stathmin: a protein with many tasks. *New biomarker and potential target in cancer. Expert Opin Ther Targets* 2011; 15:1249-66; PMID:21978024; <http://dx.doi.org/10.1517/14728222.2011.620951>
  24. Glover CE, Gurley KE, Kim K-H, Storer B, Fero ML, Kemp CJ. Endocrine dysfunction in p27Kip1 deficient mice and susceptibility to Wnt-1 driven breast cancer. *Carcinogenesis* 2009; 30:1058-63; PMID:19380520; <http://dx.doi.org/10.1093/carcin/bgp089>
  25. Chien W-M, Garrison K, Caufield E, Orthel J, Dill J, Fero ML. Differential gene expression of p27Kip1 and Rb knockout pituitary tumors associated with altered growth and angiogenesis. *Cell Cycle Georget Tex* 2007; 6:750-7; <http://dx.doi.org/10.4161/cc.6.6.3986>
  26. Brattsand G, Marklund U, Nylander K, Roos G, Gullberg M. Cell-cycle-regulated phosphorylation of oncoprotein 18 on Ser16, Ser25 and Ser38. *Eur J Biochem FEBS* 1994; 220:359-68; <http://dx.doi.org/http://dx.doi.org/10.1111/j.1432-1033.1994.tb186s32.x>
  27. Andersen SS, Ashford AJ, Tournebize R, Gavet O, Sobel A, Hyman AA, Karsenti E. Mitotic chromatin regulates phosphorylation of Stathmin/Op18. *Nature* 1997; 389:640-3; PMID:9335509; <http://dx.doi.org/10.1038/39382>
  28. Malumbres M. Physiological relevance of cell cycle kinases. *Physiol Rev* 2011; 91:973-1007; PMID:21742793; <http://dx.doi.org/10.1152/physrev.00025.2010>
  29. Chien W-M, Rabin S, Macias E, Miliani de Marval PL, Garrison K, Orthel J, Rodriguez-Puebla M, Fero ML. Genetic mosaics reveal both cell-autonomous and cell-nonautonomous function of murine p27Kip1. *Proc Natl Acad Sci U S A* 2006; 103:4122-7; PMID:16537495; <http://dx.doi.org/10.1073/pnas.0509514103>
  30. Tong W, Pollard JW. Genetic evidence for the interactions of cyclin D1 and p27(Kip1) in mice. *Mol Cell Biol* 2001; 21:1319-28; PMID:11158317; <http://dx.doi.org/10.1128/MCB.21.4.1319-1328.2001>
  31. Geng Y, Yu Q, Sicinska E, Das M, Bronson RT, Sicinski P. Deletion of the p27Kip1 gene restores normal development in cyclin D1-deficient mice. *Proc Natl Acad Sci U S A* 2001; 98:194-9; PMID:11134518; <http://dx.doi.org/10.1073/pnas.98.1.194>
  32. Malumbres M, Sotillo R, Santamaria D, Galán J, Cerezo A, Ortega S, Dubus P, Barbacid M. Mammalian cells cycle without the D-type cyclin-dependent kinases Cdk4 and Cdk6. *Cell* 2004; 118:493-504; PMID:15315761; <http://dx.doi.org/10.1016/j.cell.2004.08.002>
  33. Hu MG, Deshpande A, Schlichting N, Hinds EA, Mao C, Dose M, Hu G-F, Van Etten RA, Gounari F, Hinds PW. CDK6 kinase activity is required for thymocyte development. *Blood* 2011; 117:6120-31; PMID:21508411; <http://dx.doi.org/10.1182/blood-2010-08-300517>
  34. Delalay C, Liu L, Lee J-A, Su H, Shen F, Yang G-Y, Young WL, Ivey KN, Gao F-B. MicroRNA-9 coordinates proliferation and migration of human embryonic stem cell-derived neural progenitors. *Cell Stem Cell* 2010; 6:323-35; PMID:20362537; <http://dx.doi.org/10.1016/j.stem.2010.02.015>
  35. Scita G, Di Fiore PP. The endocytic matrix. *Nature* 2010; 463:464-73; PMID:20110990; <http://dx.doi.org/10.1038/nature08910>
  36. Draghici S, Khatri P, Tarca AL, Amin K, Done A, Voichita C, Georgescu C, Romero R. A systems biology approach for pathway level analysis. *Genome Res* 2007; 17:1537-45; PMID:17785539; <http://dx.doi.org/10.1101/gr.6202607>